Selected Results on Strong and Coulomb-Induced Correlations from the STAR Experiment

M. Šumbera for the STAR Collaboration

Nuclear Physics Institute, Academy of Sciences of the Czech Republic, 250 68 Řež, Czech Republic

Using recent high-statistics STAR data from Au+Au and Cu+Cu collisions at full RHIC energy I discuss strong and Coulomb-induced final state interaction effects on identical $(\pi - \pi)$ and non-identical $(\pi - \Xi)$ particle correlations. Analysis of $\pi - \Xi$ correlations reveals the strong and Coulomb-induced FSI effects, allowing for the first time to estimate spatial extension of π and Ξ sources and the average shift between them. Source imaging techniques provide clean separation of details of the source function and are applied to the one-dimensional relative momentum correlation function of identical pions. For low momentum pions, and/or non-central collisions, a large departure from a single-Gaussian shape is observed.

I. INTRODUCTION

Progress in understanding the space-time structure of multiparticle production via femtoscopy is currently driven by high-statistics data sets accumulated in heavy ion experiments at RHIC and SPS accelerator [1–4, 10]. In particular, an ambitious program of the STAR collaboration at RHIC exploiting good particle identification has already provided a vast variety of femtoscopic measurements in different identical and non-identical particle systems, some of which were actually measured for the first time [4]. This contribution is a progress report on two currently pursued STAR femtoscopy analyses. Both of them were introduced already at the previous WPCF meeting last year in Kroměříž [2]. The first focuses on non-identical particle correlations in rather exotic meson–baryon system $\pi^{\pm} - \Xi^{\pm}$ [5]. Previous investigations have shown that correlations among these two charged hadrons reveal not only the Coulomb but also strong final state interaction (FSI) effects [11, 12]. The order of magnitude difference in mass, plus $\Delta B=1/\Delta S=2$ gap in baryon/ strangeness quantum numbers, makes the $\pi - \Xi$ system an important tool to study the interplay between matter flow on the partonic and hadronic levels. The second analysis exploits particle correlations in a more conventional system of two identical charged pions [6]. Its aim is to understand the geometry of the source. The ultimate and rather ambitious aspiration of this project is to extract pion-pion scattering lengths. This goal will make heavy ion femtoscopic measurements fully competitive to a dedicated particle physics experiments trying to extract this important parameter of the strong interaction [3, 7, 8]. Basic prerequisites for such measurements are good knowledge of correlations due to quantum statistics and Coulomb interactions.

II. STUDYING SPACE-TIME STRUCTURE OF MULTI-STRANGE BARYON SOURCE VIA $\pi - \Xi$ CORRELATIONS

In ultra-relativistic heavy-ion collisions at RHIC, hot and dense strongly interacting matter is created exhibiting properties of de-confined partonic matter [9, 13]. Almost instantaneous equilibration of the produced matter is indicated by recent heavy flavor measurements [9, 14], and represents one

of the greatest puzzles coming from RHIC [9]. The early partonic collectivity also shows up in a subsequent evolution of the system leading to strong collective expansion of the bulk matter as demonstrated by large values of observed elliptic flow [9, 13]. These observations are further substantiated by STAR multi–strange baryon measurements showing that Ξ and Ω baryons reveal significant amount of elliptic flow which is comparable to ordinary non–strange baryons [15]. The sizable multi–strange baryon elliptic flow, which obeys constituent quark scaling [16], confirms that a substantial part of the collective motion has indeed developed prior to hadronization. This picture is also corroborated by a more recent STAR analysis of the centrality dependence of hyperon yields carried out within the framework of a thermal model [17]. The observed scaling behavior of strange baryons is consistent with a scenario of hadron formation from constituent quark degrees of freedom through quark recombination provided that the coalescence took place over a volume that is much larger than the one created in any elementary collisions.

These observations fit nicely into ideal hydrodynamic evolution starting from the system of de-confined QCD matter. However, they are also consistent with a more realistic hybrid macroscopic/microscopic transport approach [20] which takes into account the strength of dissipative effects prevalent in the latter hadronic phase of the reaction. The hybrid model calculations indicate that at the top RHIC energy the hadronic phase of the heavy-ion reactions is of significant duration (at least 10 fm/c), making hadronic freeze-out a continuous process, strongly depending on hadron flavor and momenta. In particular, heavy hadrons, which are quite sensitive to radial flow effects, obtain the additional collective push created by resonant (quasi)elastic interactions during that fairly long-lived hadronic rescattering stage [21].

It is clear that questions concerning multi–strange baryon decoupling from the hot and strongly interacting partonic/hadronic system is an interesting one, but also not an easy one to solve. Could this be provided by femtoscopy? What kind of relevant information can be obtained via low-relative-velocity correlations of multi-strange baryons with the other hadrons? Since non-identical particle correlations are sensitive not only to the extent of the source, but also to the average shift in emission time and position among differ-

ent particle species [19], the answer is affirmative. The femtoscopy of non-identical particles was already used to show that the average emission points of pions, kaons and protons produced in heavy-ion collisions at SPS and RHIC are not the same [3, 7, 10, 22, 23]. In a hydrodynamically inspired blast-wave approach [18], the mass ordering of average space-time emission points of different particle species naturally appears due to the transverse expansion of the source. This effect increases with the mass difference of the measured particle pair. Hence, studying correlations in the $\pi - \Xi$ system where the mass difference is very large should provide rather sensitive test of the emission asymmetries introduced by the transverse expansion of the bulk matter.

Moreover, in addition to the Coulomb interaction studied in the $\pi - K$ system, the small relative momentum $\pi^\pm - \Xi^\mp$ correlations may provide a clear signal of the strong interaction, revealing itself via the $\Xi^*(1530)$ resonance. Expressing particle momentum in the pair rest frame, $\mathbf{k}^* = \mathbf{p}_\pi = -\mathbf{p}_\Xi$ via pair invariant mass $M_{\pi\Xi}$ and m_π and m_Ξ

$$k^* = \frac{[M_{\pi\Xi}^2 - (m_\pi - m_\Xi)^2]^{1/2}[M_{\pi\Xi}^2 - (m_\pi + m_\Xi)^2]^{1/2}}{2M_{\pi\Xi}} \quad (1)$$

One expects the $\Xi^*(1530)$ peak to show up in the correlation function $C(k^*)$ at $k^* \approx 150$ MeV/c. Due to its rather long lifetime, $\tau_{\Xi^*(1530)} = 22 fm/c$, the resonance could also be rather sensitive to the $\pi - \Xi$ interaction during the long-lived hadronic phase. This should be investigated by both $\pi - \Xi$ femtoscopy as well as via direct measurements of $\Xi^*(1530)$ spectra. While the first signal of the Ξ^* resonance in heavy ion collision was seen in femtoscopy analysis just two years ago [24], the first preliminary STAR measurements concerning the Ξ^* spectra and their yields were presented only recently at the Quark Matter conference in Shanghai this year [25].

A. Data selection

Though in previous analyses [5, 11, 12, 24] the $\pi - \Xi$ correlations were studied for two different system d+Au and Au+Au and also at two different energies, in this contribution I will concentrate on Au+Au data at $\sqrt{(s_{NN})} = 200$ GeV from RHIC Run IV only. The data were divided into several centrality classes. During the run, the central trigger was used to enhance the fraction of the 10% most central events. Track-level cuts based on dE/dx particle identification in the STAR Time Projection Chamber were used. Pion sample momenta p_t were limited to [0.125, 1.] GeV/c. After the dE/dx cuts, the upper p_T-limit was 0.8 GeV/c and 0.6 GeV/c at $y = 0.$ and $y = 0.8$, respectively. Charged Ξs were reconstructed topologically in the p_t range [0.7, 3.] GeV/c. To increase the total number of analyzed $\pi - \Xi$ pairs in this analysis we have used a wider rapidity cut than in the previous STAR femtoscopy analyses [26]. The cut $|y| < 0.8$ instead of $|y| < 0.5$ was employed for both particle species. Total number of extracted Ξ used in this analysis are given in Table I.

TABLE I: **200 GeV Au+Au, Run IV data set**

Centrality	No. of $\Xi^\pm$	No. of Ξ^-	No. of Ξ^+
0 –10%	1084×10^3	595×10^3	489×10^3
10 – 40%	412×10^3	226×10^3	186×10^3
40 – 80%	145×10^3	79×10^3	66×10^3

B. Data analysis and corrections

The event–mixing technique was used to obtain the uncorrelated two-particle distribution in the pair rest frame. To remove spurious correlations of non-femtoscopic origin, the uncorrelated pairs were constructed from events with sufficient proximity in primary vertex position along the beam direction, multiplicity and event plane orientation variables. Pair cuts were used to remove effects of track splitting and merging. The resulting raw correlation function was then corrected for the purity of both particle species. The correction was performed individually for each bin in $\mathbf{k}^* = (k^*, cos\theta, \varphi)$ of the 3-dimensional (3D) correlation function as described bellow.

C. Pair purity analysis

The pair purity, defined as a fraction of primary $\pi - \Xi$ pairs, was calculated as a product of the particle purities of both particle species. The Ξ purity was obtained from reconstructed Ξ invariant mass plots as a function of transverse momentum. Pion purity was estimated using the parameter $\sqrt{\lambda}$ of the standard parametrization of the identical $\pi - \pi$ correlation function. The identical pion measurements were performed with the same pion cuts as those used in the $\pi - \Xi$ analysis. Since the value of the λ parameter is influenced by decays of long-lived resonances as well as by the non-Gaussian shape of the correlation function, the pion purity correction can be a significant source of systematic error.

In order to make contact with the previous STAR identical pion analyses [26] in Fig. 1, we present the k_T–dependence of parameters λ, R_{out}, R_{side} and R_{long} entering the standard out-side-long decomposition of the 3D correlation function $C(\mathbf{q}) = 1 + \lambda \cdot exp(-q_{out}^2 R_{out}^2 - q_{side}^2 R_{side}^2 - q_{long}^2 R_{long}^2)$. Here, $k_T = (|\mathbf{p}_{1T}| + |\mathbf{p}_{1T}|)/2$ is the average transverse momentum of two pions. On the same figure the ratio R_{out}/R_{side} is aso plotted. We conclude that the improved cuts used in the present analysis do not change the values of extracted parameters, but due to the increased acceptance in rapidity and transverse momenta of the pions, our analysis covers also region of lower k_T.

We have also studied the influence of electrons on the purity of the pion sample. Exclusion of pions with dE/dx within $\pm 2\sigma$ around the electron band has changed the value of the parameter λ in the k_T interval [0.15, 0.25] GeV/c by 50% at maximum. However, the other parameters characterizing the 3D correlation function of identical pions (the radii $R_{out}, R_{side}, R_{long}$) as well as the $\pi - \Xi$ correlation functions re-
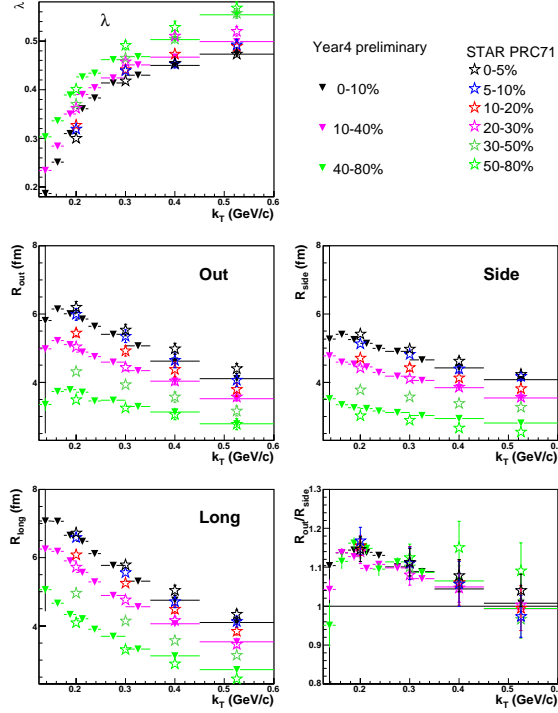
FIG. 1: (Color online) The comparison between parameters of 3D Gaussian fits to the correlation functions of identical charged pions produced in Au+Au collisions at 200 GeV. Previous [26] (open stars) and this analysis (full triangles). Error bars contain only statistical uncertainties.

mained unchanged.

D. Results in 1D source size information

The $\pi - \Xi$ correlation functions $C(k^*)$ were analyzed in the pair rest frame ($\mathbf{k}^* = \mathbf{p}_\pi = -\mathbf{p}_\Xi$). The results for unlike sign pairs are presented in Fig. 2.
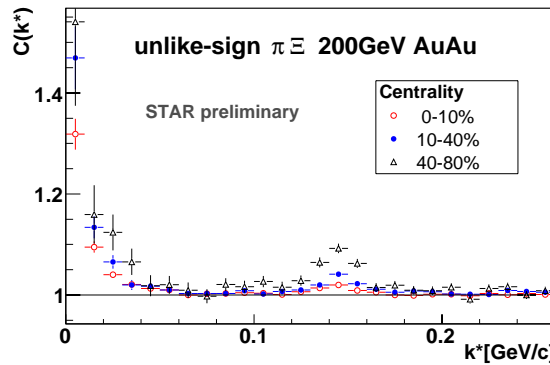

FIG. 2: (Color online) The centrality dependence of the correlation function of the combined sample of unlike-sign $\pi^\pm \Xi^\mp$ pairs .

For all centralities, the low k^* region is dominated by the Coulomb interaction. The strong interaction manifests it-

self in a peak around $k^* \approx 150$ MeV/c corresponding to the $\Xi^*(1530)$. The peak's centrality dependence clearly shows high sensitivity to the source size. Contrary to the Coulomb region, the correlation function in the resonance region does not suffer from the low statistics and can thus in principle be used to extract sizes of the sources more effectively than in the former case.

E. Results in 3D asymmetry measurement

The information about the shift in average emission points between π and Ξ can be extracted from the angular part of the 3D correlation function $C(\mathbf{k}^*) \equiv C(k^*, \cos\theta, \varphi)$.
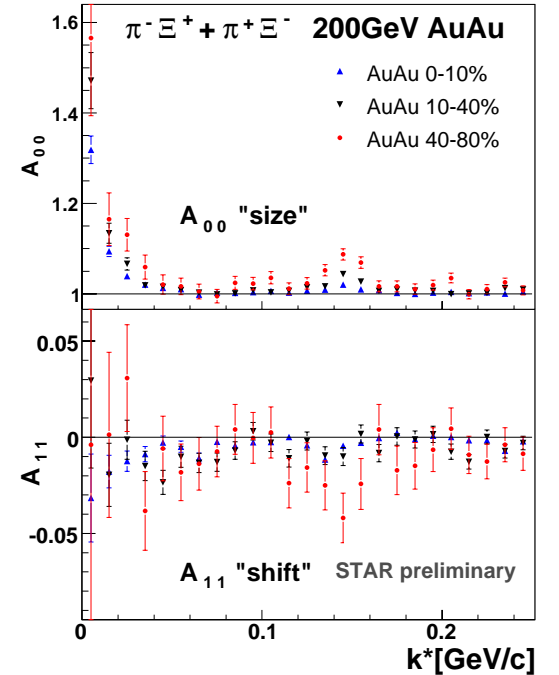

FIG. 3: (Color online) $A_{00}(k^*)$ and $A_{11}(k^*)$ coefficients of spherical decomposition for the combined sample of unlike-sign $\pi^\pm \Xi^\mp$ pairs from three different centrality bins.

The function is binned in $k^*, \cos\theta, \varphi$ with $\Delta_{\cos\theta} = \frac{2}{N_{\cos\theta}}$ and $\Delta_\varphi = \frac{2\pi}{N_\varphi}$ as the bin sizes in $\cos\theta$ and ϕ, respectively. After its decomposition into spherical harmonics [27],

$$A_{lm}(k^*) = \frac{\Delta_{\cos\theta} \Delta_\varphi}{\sqrt{4\pi}} \sum_i^{all\ bins} Y_{lm}(\theta_i, \varphi_i) C(k^*, \cos\theta_i, \varphi_i) \quad (2)$$

Symmetry further limits the number of relevant components. This is due to the fact that individual coefficients appearing in the above decomposition represent different symmetries of the source. Thus for azimuthally symmetric identical particle source at midrapidity, only A_{lm} with even values of l and m

do not vanish. On the other hand, for non–identical particle correlations the coefficients with odd values of l and m are allowed.

For both cases, the most important coefficient is $A_{00}(k^*)$ representing the angle-averaged correlation function $C(k^*)$. The latter is sensitive to the source size only, whereas in the non–identical particle case $A_{11}(k^*)$ measures a shift of the average emission point in the R_{out} direction.

The decomposition of the correlation function into spherical harmonics was used to study the centrality dependence of asymmetry in emission between pions and Ξs. The results are presented in Fig. 3. The coefficient A_{11} which is non-zero in all centrality bins clearly confirms that the average space-time emission points of pions and Ξ are not the same.

for the Ξ source as for the pions implicitly assumes significant transverse flow of Ξ. In the Coulomb region, the theoretical correlation function is in qualitative agreement with the data. Moreover, the orientation of the shift and its magnitude agrees with the scenario in which the Ξ participates in the transverse expansion. However, in the region dominated by the strong final state interaction the calculations over predict both the size and the shift coefficients.

F.   Extracting the source parameters

For further analysis we have used only the low k^* region dominated by the Coulomb interaction, excluding thus the region around the $\Xi^*(1530)$ peak (see Fig. 5).
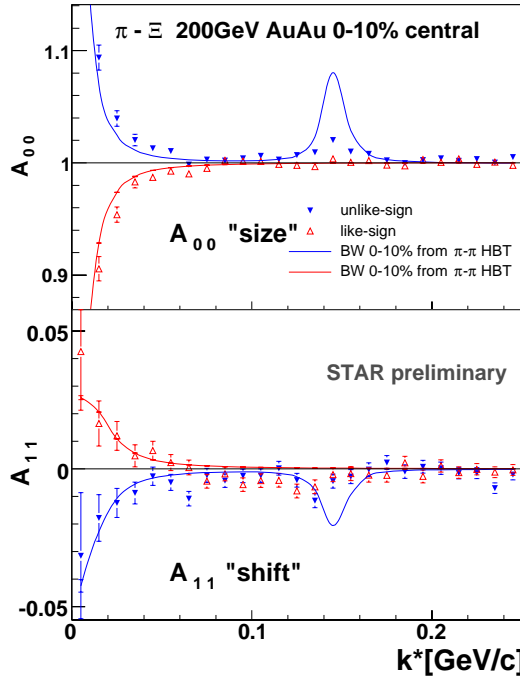

FIG. 4:   (Color online) Comparison of $A_{00}(k^*)$ and $A_{11}(k^*)$ coefficients of spherical decomposition for combined sample of unlike-sign $\pi^\pm\Xi^\mp$ pairs from 10% most central Au+Au collisions with the FSI model predictions.

In Fig. 4 the experimental results for the 10% most central, the highest statistics bin, are compared to a model calculation exploiting strong and Coulomb final state interaction [28].The theoretical correlation function was constructed from the particle emission separation distribution. For this purpose, the momenta of real particles were used. The emission coordinates of both π and Ξ were generated using the blast wave model [18]. This model, encompassing correlation between particle momenta and their space-time coordinates, was used with a single set of parameters for generating emission coordinates of both π and Ξ. These parameters were obtained from experimentally measured pion spectra and $\pi - \pi$ emission radii. Let us note that using the same set of parameters
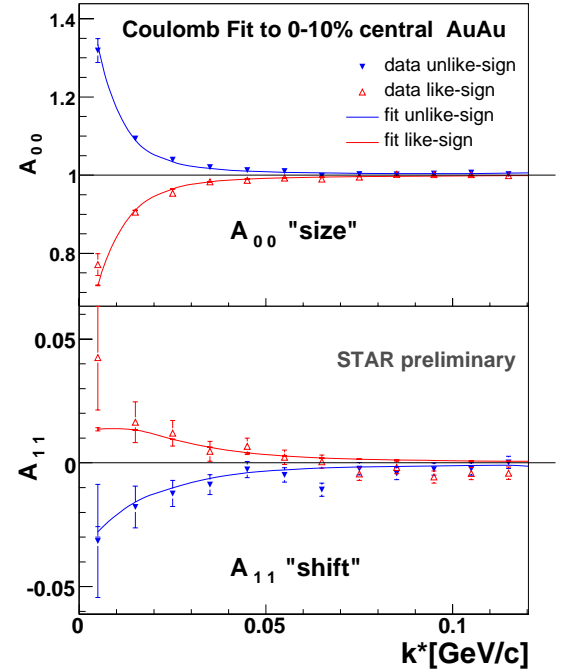

FIG. 5:   (Color online) Comparison of $A_{00}(k^*)$ and $A_{11}(k^*)$ coefficients from the spherical decomposition of the combined sample of like-sign $\pi^\pm\Xi^\pm$ and unlike-sign $\pi^\pm\Xi^\mp$ pairs from the 10% most central Au+Au collisions, along with the FSI model predictions.

The theoretical correlation function was calculated using the momentum distribution of pairs extracted from real data. The emission coordinates were randomly generated from the two-parameter source distribution constructed in the following way. For both particle species, the Gaussian shape of their source was assumed with the sources shifted in the R_{out} direction relative to each other. In the pair rest frame this can be expressed via two parameters R and Δ_{out} characterizing the pair separation distribution in Δr^*. Here, R represents the width of the Gaussian and Δ_{out} represents the shift in the R_{out} direction. Values of the source parameters were then extracted by finding a minimum value of χ^2 between theoretical and real

correlation function. Fitting was done simultaneously for like and unlike–sign correlation functions.

For the most central Au+Au collisions this method yields the first preliminary values of $R = (6.7 \pm 1.0)$ fm and $\Delta_{out} = (-5.6 \pm 1.0)$ fm. The errors are purely statistical. Systematic error studies are under way and their values are expected to be of the order of the statistical ones. In our case a negative value of the shift means that average emission point of Ξ is positioned more to the outside of the whole fire-ball than the average emission point of pion as expected in the Ξ flow scenario.

III. IDENTICAL PION CORRELATIONS

A. Motivation

In ultra–relativistic heavy–ion collisions femtoscopy can also be employed to extract information related to the strong interaction among the particles [3, 10]. In recent STAR analyses the strong FSI was studied via two–K_s^0 interferometry [29] and in proton-lambda correlations [30]. A model that takes the effect of the strong interaction into account has been used to fit the measured correlation functions. In the $p - \bar{\Lambda}$ and $\bar{p} - \Lambda$ correlations, which were actually measured for the first time, annihilation channels and/or a negative real part of the spin-averaged scattering length was needed in the FSI calculation to reproduce the measured correlation function.

At the previous WPCF meeting an ambitious proposal to exploit the correlations among identical charged pions to extract pion-pion scattering lengths was made [8]. The potential for such measurements at RHIC, and also later at the LHC stems from the fact that, compared to a dedicated particle physics experiments measuring scattering lengths parameters a_0^0 and a_0^2 like BNL-E865 [31] or Dirac [32], heavy ion experiments provide a much larger number of pion pairs at small relative momenta in a single event plus very large data samples ($10^7 - 10^9$ events). The real challenge when studying the strong interaction among identical charged pions then is to beat down all systematical errors pertinent to the ultra–relativistic heavy ion collisions environment. Coulomb interaction, pion purity and geometry of the pion source need to be kept under control. Varying the source size (k_T or centrality) may provide a good handle on this.

In particular, the bias arising from the frequently used Gaussian assumption of the source shape needs to be addressed. Using the high statistics sample of Au+Au events from the STAR experiment at RHIC's highest energy accumulated during the run IV, it was found that for all k_T and centrality bins the Lévy stable source parametrization does not bring an advantage in describing the detailed shape of measured three-dimensional correlation function [6].

The next step in this direction is to exploit the model-independent imaging technique of Brown and Danielewicz [33, 34] and reconstruct the source itself. This is done via inverting Koonin-Pratt equation (see e.g. [1]):

$$C(q) - 1 = 4\pi \int K_0(q,r)S(r)r^2dr$$

$$K_0(q,r) \equiv \frac{1}{2} \int (|\Phi(\mathbf{q},\mathbf{r})|^2 - 1)d(cos\theta_{\mathbf{q},\mathbf{r}})$$

$$q = \frac{1}{2}\sqrt{-(p_1 - p_2)^2}\,, \qquad (3)$$

which expresses the 1D correlation function $C(q)$ in terms of the probability $S(r)$ to emit a pair of particles at a separation r in the c.m. frame. $S(r)$ is usually called the source function. All FSI is encoded in the (angle averaged) final state wave function $\Phi(\mathbf{q},\mathbf{r})$ describing the propagation of the pair from a relative separation of $\mathbf{r}$ in the pair c.m. to the detector with relative momentum $\mathbf{q}$. The angle between vectors $\mathbf{q}$ and $\mathbf{r}$ is denoted by $\theta_{\mathbf{q},\mathbf{r}}$. The procedure to extract $S(r)$ via inversion of Eq. 3 is given in [34].

B. Testing the inversion procedure

To test reproducibility of he original source function by the imaging procedure we have generated Bose-Einstein (B-E) correlated and Coulomb interacting pion pairs. The momentum spectra of the pions were obtained from the 10% most central Au+Au RQMD generated events at $\sqrt{s_{NN}}$=200 GeV. The pions coordinates were randomly sampled from an isotropic 3D Gaussian distribution with the radius R=5 fm. The instantaneous emission δτ=0 of particles was assumed. Using pion momenta and their coordinates the B-E correlations and Coulomb FSI were introduced using the procedure described in [36]. Results for correlations and source functions are displayed on Fig. 6. In order to compare with the input Gaussian source the extracted source function was fitted with the Gaussian distribution again:

$$g(r,R) = \frac{\lambda}{(2\sqrt{\pi}R)^3}e^{-\frac{r^2}{4R^2}} \qquad (4)$$

Let us note that the r^2-weighting of $S(r)$ appearing in the normalization condition of the source function:

$$4\pi \int_0^\infty S(r)r^2dr = \lambda \qquad (5)$$

makes the normalization constant λ more sensitive to the behavior of $S(r)$ at $r \gg R$ than one would naively expect. Since the latter is determined by the imaging from values of the correlation function $C(q)$ at very small q, fulfilment of the above normalization condition using data with limited statistics in the low q bins may be hard to achieve. This may explain why values of the extracted parameters R and λ from the single-Gaussian fit were found to be smaller than the input ones. While for R the discrepancy is about 4% for λ it is almost 25%.

C. 1D imaging analysis of the pion source from Au+Au and Cu+Cu collisions

The same data set of Au+Au events from Run IV, used in the previously described $\pi - \Xi$ correlation analysis, was also
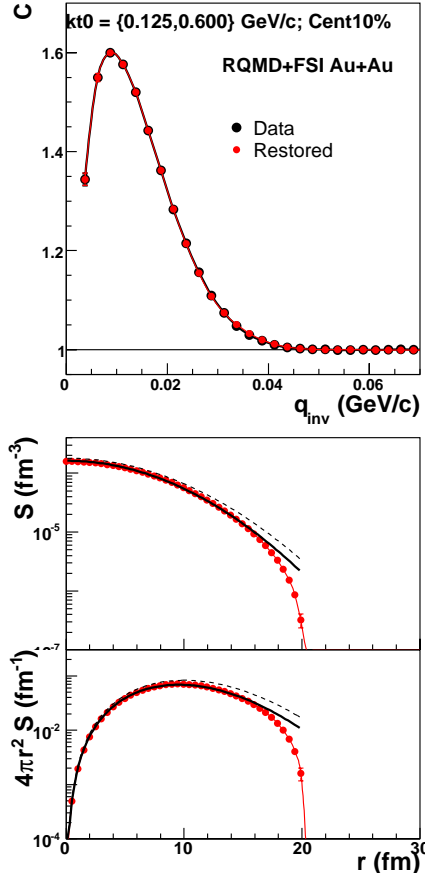
FIG. 6: (Color online) The 1D imaging analysis of an isotropic Gaussian source using pion momentum spectra from RQMD simulating the 10% most central Au+Au collisions at $\sqrt{s_{NN}}$ =200 GeV. Top: original (black filled circles) and restored by imaging technique (red filled circles) correlation function $C(q)$. To guide the eye the data points are connected by a smooth line of the same color. Middle: 1D source function $S(r)$ (red filled circles). The full black line represents the result of a single-Gaussian fit to $S(r)$, dashed line - input Gaussian distribution. Bottom: $4\pi r^2 S(r)$.
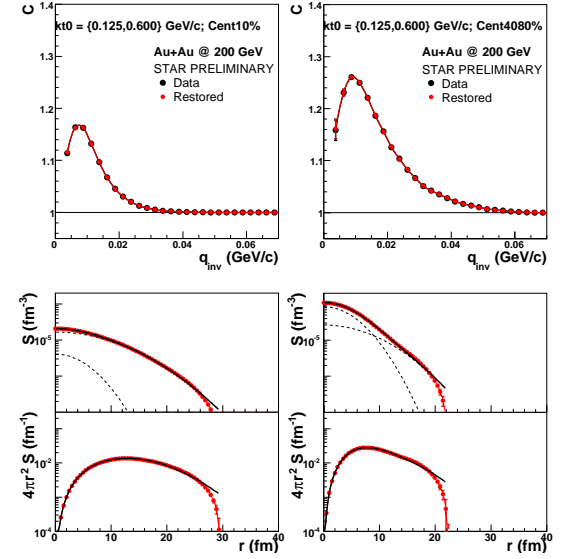

FIG. 7: (Color online) 1D imaging analysis of identical charged pions from Au+Au collisions at $\sqrt{s_{NN}}$ =200 GeV. Results are shown for the 10% most central (the left panel) and for peripheral(centrality 40-80%) collisions (the right panel). Top: the measured correlation function C(q) (black filled circles), restored correlation function from imaging technique (red filled circles). To guide the eye the data points are connected by a smooth line of the same color. Middle: 1D source function $S(r)$ (red filled circles). The full black line represents the result of a double-Gaussian fit to $S(r)$. Two dashed lines show contribution of each of two Gaussians. Bottom: $4\pi r^2 S(r)$: (red filled circles). Full black line represents result of a double-Gaussian fit.

used for the reconstruction of the pion source. The second data set employed in the imaging analysis consists of about 8 million Cu+Cu minimum bias events at $\sqrt{s_{NN}}$=200 GeV accumulated during the Run V. Selected results from 1D imaging analysis of the pion source using centrality selected Au+Au and Cu+Cu events are displayed on Fig. 7 and 8, respectively.

Compared to the model example discussed in the previous paragraph the extracted source functions now develop long tails [35] and cannot thus be described by a single Gaussian distribution. The only exception are the data from the 10% most central Au+Au collisions (Fig. 7.) To account for the observed behavior we use the simplest extension of Eq. 4 and assume that the source function contains contributions from two Gaussians. While the first Gaussian $g(r,R_1)$ contributing with fraction $(1-\alpha)$ is responsible for the long tails the second one $g(r,R_2)$ contributing with weight α of width the

$R_2 < R_1$ describes the source function at small r. The double Gaussian distribution:

$$G(r,R_1,R_2) = (1-\alpha)g(r,R_1) + \alpha g(r,R_2), R_1 > R_2 \qquad (6)$$

now seems to describe data quite well. Comparing Au+Au to Cu+Cu collisions of the same centrality we conclude that the long tails are more pronounced for the smaller system.

All source functions presented so far were obtained from data integrated over the whole range of average pair transverse momenta k_T= [0.125, 0.600] GeV/c. In the following I will present results showing how much the observed departure from a single Gaussian shape depends on particle transverse momenta.

Such an analysis was performed and is displayed in Figs. 9-11. While for Au+Au collisions the statistics allowed us to use 9 bins in k_T for Cu+Cu we have used only 4 bins. In Fig. 9 the lowest k_T= [0.125, 0.250] GeV/c and the highest k_T= [0.450, 0.600] GeV/c bins from Cu+Cu 10% most central collisions are compared. We see that the long tail present in the lowest k_T bin, which is characterized by the Gaussion with the width $R \approx 7$ fm, completely disappears from the highest k_T bin.

Figures 10 and 11 show the k_T-dependence of the double Gaussian fit parameters for Cu+Cu and Au+Au collisions at three different centralities. We observe that with increasing k_T, the contribution of the second Gaussian is less and less
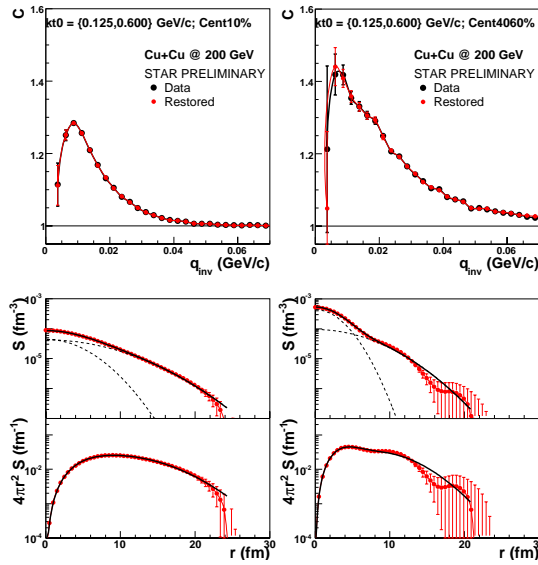
FIG. 8: (Color online) 1D imaging analysis of identical charged pions from Cu+Cu collisions at $\sqrt{s_{NN}}$ =200 GeV. Results are shown for the 10% most central (the left panel) and for peripheral (centrality 40-60%) collisions (the right panel). Top: C(q). Middle: 1D source function $S(r)$. Bottom: $4\pi r^2 S(r)$. Labels are same as on Fig. 7.
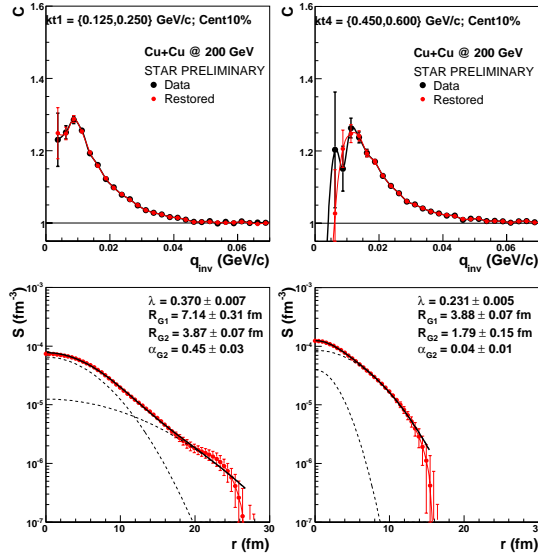

FIG. 10: (Color online) The k_T-dependence of source parameters of identical charged pions from Cu+Cu collisions at $\sqrt{s_{NN}}$=200 GeV taken at three different centralities: 0-10% - full red circles, 10-40% - full blue squares, 40-60% - full black triangles.

FIG. 9: (Color online) The 1D imaging analysis of identical charged pions from the 10% most central Cu+Cu collisions at $\sqrt{s_{NN}}$=200 GeV. Results are shown for the lowest (the left panel) and for the highest (the right panel) k_T-bin. Top: correlation function C(q). Middle: 1D source function $S(r)$ Bottom: $4\pi r^2 S(r)$. Labels are same as on Fig. 7.

FIG. 11: (Color online) The k_T-dependence of source parameters of identical charged pions from Au+Au collisions at $\sqrt{s_{NN}}$=200 GeV taken at three different centralities: 0-10% - full red circles, 10-40% - full blue squares, 40-80% - full black triangles.

prominent. This behavior is more pronounced in Cu+Cu collisions. Let us note that the long tails observed in the low-k_T bins may then indicate an important role played by the pions from long-lived resonance decays. An interesting observation
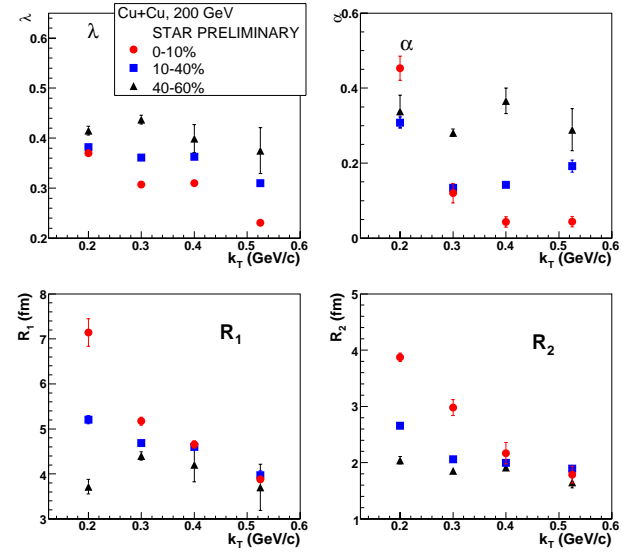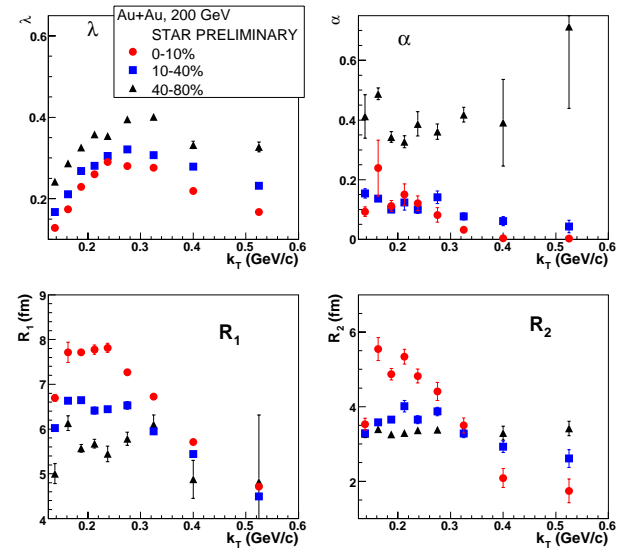
which may have some relevance to the observed behavior regarding the random walk nature of particle freeze-out in coordinate space was made by T. Csörgő at this meeting [37].

IV. SUMMARY

High-statistics STAR data from Au+Au and Cu+Cu colli-sions taken at full RHIC energy and three different centralities were used to discuss recent progress in identical $(\pi - \pi)$ and non-identical $(\pi - \Xi)$ particle femtoscopy. In the $\pi - \Xi$ system the strong and Coulomb-induced FSI effects were observed, making it possible for the first time to estimate the average shift and width between π and Ξ source. The 1D imaging of the identical pion source reveals a significant departure from a single Gaussian shape. The observed long tails, which could be fairly well described by allowing for the second Gaussian, are more pronounced for the sources produced at large impact parameters. The effect is stronger for Cu+Cu than for Au+Au collisions. For all centralities and both colliding systems the highest departure from a single Gaussian shape is observed for sources emitting particle with a small average pair transverse momenta k_T. For the highest analyzed k_T the source is to a good approximation a single Gaussian.

Acknowledgements

[1] M. A. Lisa, S. Pratt, R. Soltz, and U. Wiedemann, Ann. Rev. Nucl. Part. Sci. **55**, 357 (2005) [arXiv:nucl-ex/0505014].

[2] Proc. XXXV Int. Symp. on Multiparticle Dynamics (ISMD 2005), Kroměříž, Czech Republic, August 9-15, 2005 and of the Workshop on Particle Correlations and Femtoscopy (WPCF 2005), Kroměříž, Czech Republic, August 15-17, 2005. Edited by V. Šimák, M. Šumbera, Š. Todorova, B. Tomášik, AIP Conference Proceedings 828 (2006), ISBN 0-7354-0320-1.

[3] R. Lednický, ibid, p. 423 (2006).

[4] M. Lisa, ibid, p. 226 (2006).

[5] P. Chaloupka, ibid, p. 610 (2006).

[6] M. Bysterský, ibid, p. 205 (2006) [arXiv:nucl-ex/0511053].

[7] R. Lednický, Proc. CIPPQG'01, Palaiseau, France, arXiv:nucl-th/0112011; Phys. Atom. Nucl. **67**, 72 (2004).

[8] M. Bysterský and F. Retiere: "Measuring scattering length at STAR," unpublished talk at WPCF 2005. Available at http://www.particle.cz/conferences/wpcf2005/talks/retiere.ppt.

[9] Proc. 18th Int. Conf. on Ultra-Relativistic Nucleus-Nucleus Collisions, Budapest, Hungary, 4-9 August, 2005, edited by T. Csörgő, G. Dávid, and P. Lévai, Nucl. Phys. A **774** (2006).

[10] R. Lednický, ibid, p. 189 (2006).

[11] P. Chaloupka, ibid, p. 603 (2006).

[12] P. Chaloupka, Proc. SQM 2006 Int. Conf on Strangeness in Quark Matter, University of California Los Angeles, March 26-31, 2006, edited by K. Barish, H. Z. Huang, J. Kapusta, G. Odyniec, J. Rafelski, and C. A. Whitten Jr., J. Phys. G **32**, S537 (2006).

[13] J. Adams et al. [STAR Collaboration], Nucl. Phys. A **757**, 102 (2005).

[14] B. I. Abelev et al. [STAR Collaboration], arXiv:nucl-ex/0607012.

[15] J. Adams et al. [STAR Collaboration], Phys. Rev. Lett. **95**, 122301 (2005).

[16] D. Molnar and S. A. Voloshin, Phys. Rev. Lett. **91**, 092301 (2003), R. J. Fries, B. Muller, C. Nonaka, and S. A. Bass, Phys. Rev. Lett. **90**, 202303 (2003).

[17] J. Adams et al. [STAR Collaboration], arXiv:nucl-ex/0606014.

[18] F. Retiere and M. A. Lisa, Phys. Rev. C **70**, 044907 (2004).

[19] R. Lednicky, V. L. Lyuboshits, B. Erazmus, and D. Nouais, Phys. Lett. B **373**, 3034 (1996).

[20] C. Nonaka and S. A. Bass, Phys. Rev. C **75**, 014902 (2007).

[21] U. W. Heinz, J. Phys. G **31**, S717 (2005).

[22] C. Blume et al. [NA49 Collaboration], Nucl. Phys. A **715**, 55 (2003).

[23] J. Adams et al. [STAR Collaboration], Phys. Rev. Lett. **91**, 262302 (2003).

[24] P. Chaloupka [STAR Collaboration], Nucl. Phys. A **749**, 283 (2005).

[25] R. Witt, talk at 19th Int. Conf. on Ultra–Relativistic Nucleus–Nucleus Collisions, Shanghai, China, November 14-20, 2006, arXiv:nucl-ex/0701063.

[26] J. Adams et al. [STAR Collaboration], Phys. Rev. C **71**, 044906 (2005).

[27] Z. Chajecki, T. D. Gutierrez, M. A. Lisa, and M. Lopez-Noriega [the STAR Collaboration], arXiv:nucl-ex/0505009.

[28] S. Pratt and S. Petriconi, Phys. Rev. C **68**, 054901 (2003).

[29] B. I. Abelev [STAR Collaboration], Phys. Rev. C **74**, 054902 (2006); S. Bekele and R. Lednicky, "Neutral Kaon Correlations in $\sqrt{s_{NN}} = 200$ GeV Au+Au collisions at RHIC", Proc. WPCF 2006.

[30] J. Adams et al. [STAR Collaboration], arXiv:nucl-ex/0511003.

[31] S. Pislak et al. [BNL-E865 Collaboration], Phys. Rev. Lett. **87**, 221801 (2001).

[32] B. Adeva et al. [DIRAC Collaboration], Phys. Lett. B **619**, 50 (2005).

[33] D. A. Brown and P. Danielewicz, Phys. Lett. B **398**, 252 (1997).

[34] D. A. Brown and P. Danielewicz, Phys. Rev. C **57**, 2474 (1998).

[35] S. S. Adler et al. [PHENIX Collaboration], arXiv:nucl-ex/0605032.

[36] R. Lednický and V.L. Lyuboshits, Yad. Fiz. **35**, 1316 (1982) [Sov. J. Nucl. Phys. **35**, 770 (1982)]. Fortran program provided by R. Lednický.

[37] M. Csanad, T. Csörgő, and M. Nagy, arXiv:hep-ph/0702032.